

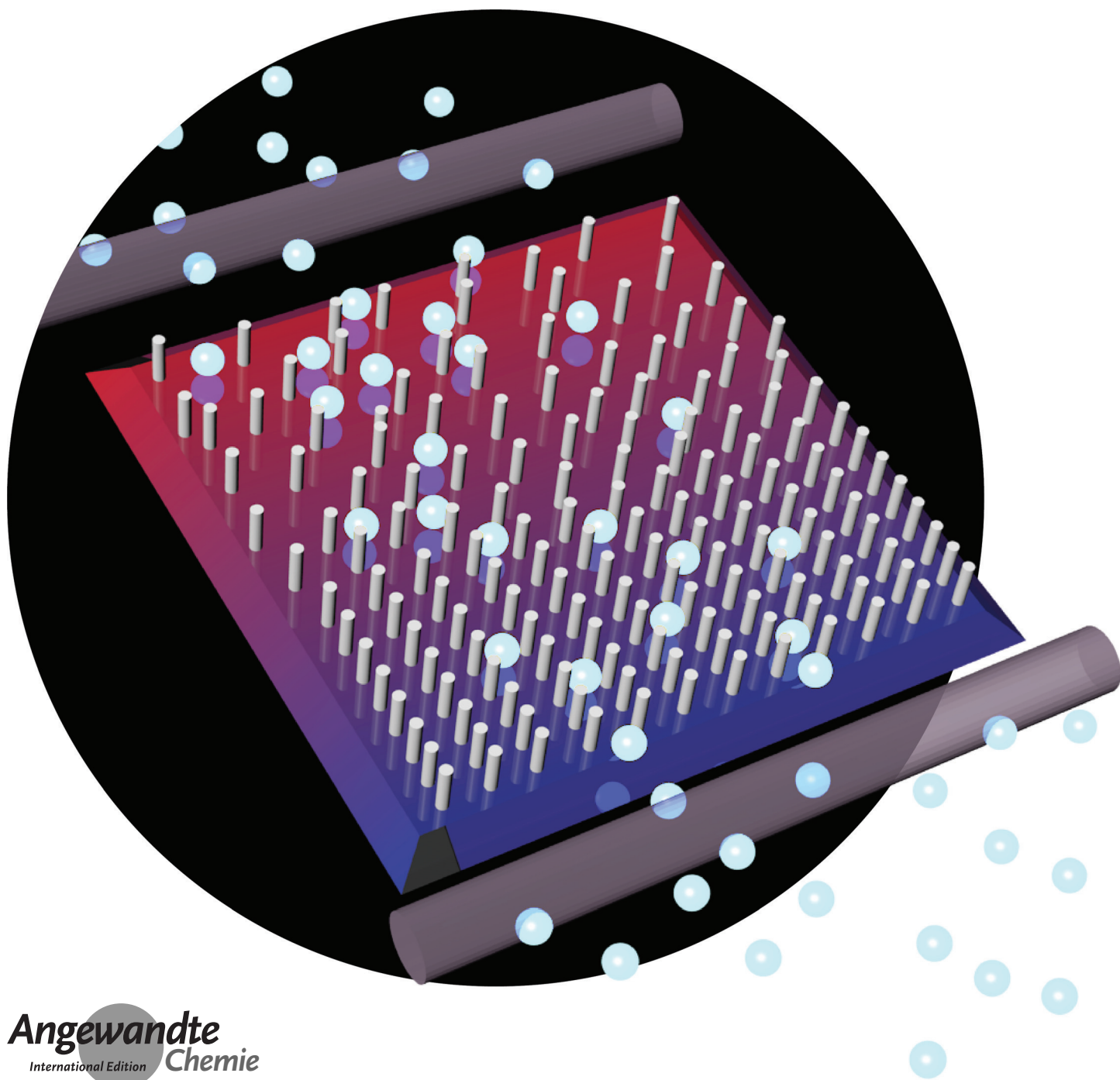
NMR Spectroscopy

International Edition: DOI: 10.1002/anie.201511539

German Edition: DOI: 10.1002/ange.201511539

Nondisruptive Dissolution of Hyperpolarized ^{129}Xe into Viscous Aqueous and Organic Liquid Crystalline Environments

Ashley E. Truxal, Clancy C. Slack, Muller D. Gomes, Christophoros C. Vassiliou, David E. Wemmer, and Alexander Pines*



Abstract: Studies of hyperpolarized xenon-129 ($hp\text{-}^{129}\text{Xe}$) in media such as liquid crystals and cell suspensions are in demand for applications ranging from biomedical imaging to materials engineering but have been hindered by the inability to bubble Xe through the desired media as a result of viscosity or perturbations caused by bubbles. Herein a device is reported that can be reliably used to dissolve $hp\text{-}^{129}\text{Xe}$ into viscous aqueous and organic samples without bubbling. This method is robust, requires small sample volumes ($< 60\ \mu\text{L}$), is compatible with existing NMR hardware, and is made from readily available materials. Experiments show that Xe can be introduced into viscous and aligned media without disrupting molecular order. We detected dissolved xenon in an aqueous liquid crystal that is disrupted by the shear forces of bubbling, and we observed liquid-crystal phase transitions in (MBBA). This tool allows an entirely new class of samples to be investigated by hyperpolarized-gas NMR spectroscopy.

Hyperpolarized xenon-129 ($hp\text{-}^{129}\text{Xe}$) has proven to be an effective reporter for many biological and chemical systems, including in vivo medical imaging.^[1] Xenon NMR is also useful in material science as a highly sensitive, inert probe for the properties of liquid-crystal (LC) phases, nanochannels, and porous structures, and as a real-time reporter for the progress of chemical processes.^[2] Anisotropic chemical environments, such as LC phases, can cause substantial shielding anisotropy in the xenon chemical shift tensor.^[3] This anisotropy is due to deformation of xenon's electron cloud caused by the ordering of molecules near it. In an isotropic environment, unrestricted molecular tumbling averages this contribution to zero. When molecular motion is constrained by electrostatic, steric, or other noncovalent interactions in an ordered phase, an anisotropic contribution, proportional to the degree of LC order, adds to the observed ^{129}Xe chemical shift. For thermotropic LCs like *N*-(4-methoxybenzylidene)-4-butylaniline (MBBA), the degree of positional ordering and angle of the director axis with respect to the external field can be deduced from the xenon chemical shift anisotropy through variable-temperature studies.^[2a]

In addition to materials applications, the ability to study LC phases by using $hp\text{-}^{129}\text{Xe}$ NMR spectroscopy will be advantageous for biosensing. $Hp\text{-}^{129}\text{Xe}$ has proven effective for detection and analysis of a growing number of biological samples, including gas vesicles, bacterial spores, bacterio-

phage, proteins, and cells.^[4] Biological processes, such as enzymatic cleavage and protein complex formation, have also been monitored by xenon NMR.^[5] In a number of these studies, $hp\text{-}^{129}\text{Xe}$ associated with targeted cryptophane conjugates has modest changes in chemical shift upon binding to biological targets. The introduction of orientation-dependent interactions in an ordered environment is expected to enhance the shift change associated with xenon binding events. Increasing the separation of bound and unbound sensor resonance signals will allow better contrast, and faster, more sensitive biosensing.

NMR studies with $hp\text{-}^{129}\text{Xe}$ require rapid delivery to avoid loss of signal through relaxation before detection. $Hp\text{-}^{129}\text{Xe}$ has usually been introduced into samples through bubbling or shaking of Xe gas mixtures with the solution of interest, but these approaches are incompatible with viscous and/or easily damaged solutions such as liquid crystals or cell suspensions.^[4,5b-d,6] An alternate approach has been to flow the solution of interest around Xe-permeable membrane tubes pressurized externally with $hp\text{-}^{129}\text{Xe}$, then into the NMR probe, for example, over alginate beads containing cells.^[6] This family of setups relies on the ability to pre-dissolve $hp\text{-}^{129}\text{Xe}$ into a flowing transport medium that is later added to a sample of interest in the magnet.^[7] Unfortunately, this approach is also incompatible with highly viscous or shear-sensitive solutions.

By contrast, the dissolution of xenon into stationary liquids has been accomplished in two different ways: first, by pressurization with thermally polarized (TP), isotopically enriched, pure xenon sources,^[3,5a,8] and second, by using porous polypropylene hollow membrane fibers.^[9] Until now, the only way to visualize viscous media by ^{129}Xe NMR spectroscopy was through TP-xenon pressurization, which is costly and often time consuming compared to $hp\text{-}^{129}\text{Xe}$ experiments. In the latter case, the solutions studied were neither viscous nor sensitive to agitation. We have also noted that polypropylene hollow fibers tend to rupture and break easily compared to silicone, often leading to the generation or trapping of bubbles in viscous samples.

To enable $hp\text{-}^{129}\text{Xe}$ studies of viscous, ordered, or otherwise mechanically sensitive solutions, we developed a new method for direct dissolution of $hp\text{-}^{129}\text{Xe}$ into any solution through silicone gas-exchange membranes, in situ in the NMR spectrometer. This approach is compatible with existing NMR probes. The membrane device, circa 4 mm in diameter, fits into a standard 5 mm NMR tube and requires less than 60 μL of sample. Samples are recoverable and no loss of performance was detected after repeated introduction and removal of samples.

A schematic of the assembled setup is shown in Figure 1. A detailed description of the setup and the experimental procedure using this device can be found in the Supporting Information. In short, the sample is injected by syringe through a polyimide fluid inlet tube and into the membranes by means of a plastic flow director cap.

Compared to previous xenon dissolution work, the positions of the $hp\text{-}^{129}\text{Xe}$ gas and sample are reversed in our assembly: where other devices had xenon flowing from the inner volume of hollow fiber membranes to a surrounding

[*] A. E. Truxal, C. C. Slack, M. D. Gomes, Dr. C. C. Vassiliou, Prof. Dr. D. E. Wemmer, Prof. Dr. A. Pines
Department of Chemistry, University of California
Berkeley, CA 94720-1460 (USA)
E-mail: pines@berkeley.edu

A. E. Truxal, C. C. Slack, M. D. Gomes, Dr. C. C. Vassiliou, Prof. Dr. A. Pines
Material Science Division, Lawrence Berkeley National Laboratory
Berkeley, CA 94720-1460 (USA)
Prof. Dr. D. E. Wemmer
Molecular Biophysics and Integrated Bioimaging Division
Lawrence Berkeley National Laboratory
Berkeley, CA 94720-1460 (USA)

Supporting information for this article can be found under:
<http://dx.doi.org/10.1002/anie.201511539>.

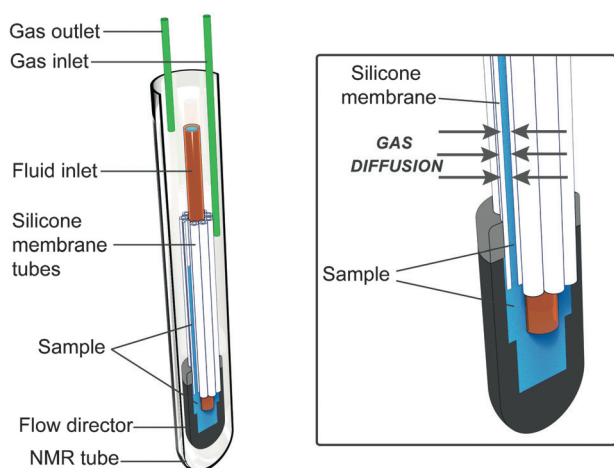


Figure 1. Cut-away view of the membrane device showing the internal design of membrane fibers and the flow director. The sample (blue) is injected into the central polyimide fluid inlet tube (orange) and into the membranes by means of the flow director, which caps the bottom of the prototype. Xenon gas is introduced into and removed from the surrounding space through the gas inlet and outlet capillaries (green).

sample liquid, we elected to place the sample inside the hollow fibers surrounded by $hp\text{-}^{129}\text{Xe}$ gas.^[7,9] By placing the sample inside the membranes and selectively exciting the dissolved xenon resonance signal, we utilize our pool of hyperpolarized xenon gas more efficiently, compared to previous membrane-based dissolution setups, while also requiring significantly less sample compared to typical bubbling experiments.

^{129}Xe spectra acquired using this system confirm the dissolution of xenon inside isotropic and ordered nematic solutions. The organic LC in this study was MBBA, which is uniaxial and thermotropic. Weakly aligning, uniaxial pf1 bacteriophage was studied as an example of an aqueous LC medium. Variable-temperature studies of MBBA and variable-concentration studies of solutions of the bacteriophage pf1 were carried out by using ^2H and ^{129}Xe NMR spectroscopic experiments to confirm ordering and to demonstrate the utility of our approach for introducing $hp\text{-Xe}$ into previously inaccessible systems.

We used both aqueous and organic liquid crystals to serve as examples of viscous and aligned media, demonstrating the broad applicability of the device. Pf1 bacteriophage and MBBA were used as model samples because neither can be probed by $hp\text{-}^{129}\text{Xe}$ using bubbling or “shake-and-bake” experiments (which consist of pressurizing then physically agitating the sample to encourage mixing of the gas and solution). Both MBBA and pf1 are too viscous for bubbling to effectively dissolve xenon in a 5 mm tube. Shake-and-bake experiments fail because of poor mixing as well as the long times required to re-establish macroscopic order after mixing. Bacteriophage pf1 further serves as a model for relatively fragile biological samples, since shear forces caused by shaking or bubbling can damage it.^[10] Since the ability of bacteriophage pf1 to form ordered phases relies on its structure being intact, the observation of unperturbed molec-

ular ordering by pf1 indicates that this setup should be useful to study other delicate samples, such as living cells.

Molecular ordering was monitored by ^2H NMR spectroscopy. Deuterium, a nucleus with $\text{spin} = 1$, has a quadrupole moment and yields a distinct peak splitting in aligned media. Observation of ^2H splittings confirmed that alignment was maintained in both MBBA and pf1 during the introduction of xenon.

A resonance signal attributable to xenon inside the walls of the silicone membranes consistently appeared at around $\delta = 195$ ppm in ^{129}Xe NMR spectra (Figure 2; Figure 3). The xenon-in-silicone signal moved an average 0.28 ppm/ $^{\circ}\text{C}$

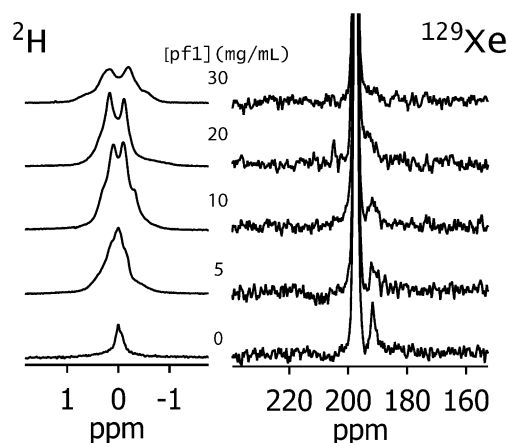


Figure 2. ^2H and ^{129}Xe NMR spectra of 10% D_2O in 0–30 mg mL^{-1} pf1 phase. ^2H quadrupolar splitting indicates increasing ordering of D_2O molecules as the phage concentration increases. The signal for dissolved ^{129}Xe at $\delta \approx 191$ ppm broadens and coalesces with the silicone signal as phage concentrations increase.

upfield for aqueous samples and 0.23 ppm/ $^{\circ}\text{C}$ upfield for organic samples. This linear, upfield trend has also been observed for xenon adsorbed in polydimethylsiloxane (PDMS).^[11] Dissolution of hyperpolarized xenon in aqueous and organic liquids of both low and high viscosity inside the membranes occurred in less than a minute, as monitored by the time evolution of signals for dissolved xenon in arrayed single-shot spectra.

The resonance signal for dissolved xenon in aqueous solution was detected near $\delta = 191$ ppm (Figure 2, right), consistent with the value from bubbling xenon directly into solution. Viscous aqueous samples of pf1 bacteriophage provided weaker signals than the MBBA, due, in part, to the lower solubility of xenon in water.^[12] Nevertheless, the increase in ^2H quadrupolar splittings from D_2O , reflecting increased order of the D_2O ^[13] with increasing concentrations of phage (Figure 2, left), demonstrate that the ordering remains unperturbed inside the membranes. Recent theoretical work supports that the order we observe inside the membranes is due to external-field-induced alignment and not wall interactions.^[14] Drawing from a study that applied thermally polarized xenon to an aqueous, lyotropic LC, we believe the significant broadening of the ^2H resonance signals with increasing phage concentration (Figure 2) may reflect a collapse of the liquid-crystal phase.^[8b]

MBBA has a well-characterized nematic-to-isotropic phase transition,^[15] with the temperature at which this phase transition occurs heavily dependent on the identity and amount of solute dissolved in the MBBA.^[16] The ^2H NMR spectra (Figure 3, top) show quadrupolar splittings of $[\text{D}_6]\text{benzene}$ at low temperatures but which disappear between 35 °C and 40 °C, demonstrating a loss of order. This interval is consistent with previous work on similar samples.^[16]

^{129}Xe has a spin of 1/2 and, therefore, does not have a quadrupole moment, but the chemical shift is sensitive to phase transitions in ordered media. A linear variation in the xenon-in-MBBA chemical shift occurs because of the increasing temperature, with an abrupt chemical shift change $\Delta\delta = 12.4$ ppm between 35 °C and 40 °C (Figure 3, bottom). This marked increase in shielding indicates a positive anisotropy of diamagnetic susceptibility, a known quality of MBBA,^[17] and a common characteristic of liquid crystals whose director axes are parallel to the external field.^[2a]

Both MBBA and pf1 bacteriophage are highly viscous samples into which xenon gas cannot be introduced by bubbling or shaking methods, previously precluding hyperpolarized gas experiments. With our device, it is now possible

to obtain high quality hyperpolarized xenon NMR spectra of these viscous solutions, or others prone to damage by agitation, in a moderate timeframe without the requirement of isotopically enriched xenon sources, liquid flow, or shaking.

We have developed the first robust method for dissolving $\text{hp-}^{129}\text{Xe}$ directly into viscous liquids without bubbling, enabling completely new types of hyperpolarized gas studies. Proof-of-concept experiments demonstrated the quantitative abilities of this method in both aqueous and organic solutions, specifically in the detection of the nematic-isotropic phase transition of a thermotropic liquid crystal. These results mark the potential for new studies of $\text{hp-}^{129}\text{Xe}$ in viscous and other anisotropic media, including those with cells, protein solutions, liquid crystals, and polymers. This system also allows direct introduction of other gases into the sample, including oxygen and carbon dioxide for cell suspensions.

Experimental Section

Details of membrane assembly construction and the experimental setup can be found in the Supporting Information.

Sample preparation: Solutions of $[\text{D}_6]\text{benzene}$ (Isotec; 3% by volume) in MBBA (Sigma-Aldrich) were used for studies of solute ordering by ^2H and ^{129}Xe NMR experiments inside the membranes. Solutions of D_2O (Sigma-Aldrich; 10% by volume) in 0–30 mg mL^{-1} pf1 bacteriophage (Asla Biotech) were prepared by diluting the phage with deionized water. All phage experiments were carried out at 15 °C.

NMR experiments: Hyperpolarized ^{129}Xe was generated by spin-exchange optical pumping of a gas mixture of 2% Xe, 10% N_2 , and 88% He (Airgas) using a homebuilt polarizer. $\text{Hp-}^{129}\text{Xe}$ flowed directly into 5 mm or 10 mm valved NMR tubes for the pf1 phage and the MBBA samples, respectively, at 0.2 slpm (slpm = standard liter per minute) held at 240 kPa for all experiments. All NMR data were acquired on a 9.4 T magnet with a Varian VNMRs console.

^{129}Xe NMR experiments were carried out using a multiple-acquisition, selective-excitation sequence with a center frequency at 17 kHz relative to the resonance frequency of ^{129}Xe gas at 9.4 T (≈ 110 MHz) and a bandwidth of 5 kHz to 8 kHz. Between 4 and 8 transients were collected per repetition, followed by a 10 s delay during which hp-Xe inside the phantom was replenished. A fitting with a glass capillary allowed the flow of hyperpolarized xenon from a homebuilt polarizer to the bottom of the phantom. Spectra were referenced to the Xe gas signal.

^2H NMR data were acquired with xenon flowing through the system to assure that observed ordering was maintained in the presence of xenon. A basic pulse-acquire sequence with a pulse length of 17.5 μs (5 mm probe) or 34 μs (10 mm probe) and a 1 s delay between transients was used. In the variable temperature studies of MBBA, temperatures were swept from low to high. An equilibration time of about 40 min was used after each temperature increase to ensure equilibration inside the membranes such that ^2H quadrupolar splittings remained constant.

Acknowledgements

This work was supported by the U.S. Department of Energy, Office of Science, Basic Energy Sciences, Materials Sciences and Engineering Division, under Contract No. DE-AC02-05CH11231. C.C.S. is also supported by a National Science Foundation Graduate Research Fellowship under Grant No. DGE-1106400.

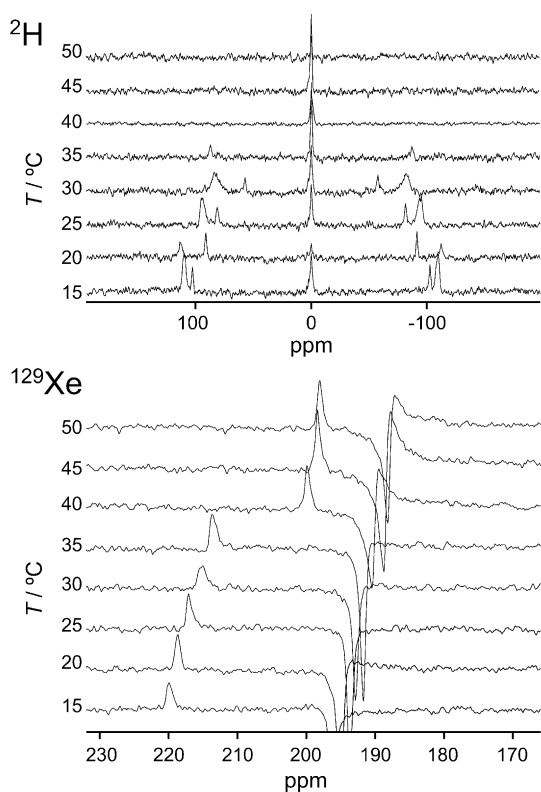


Figure 3. ^2H (top) and ^{129}Xe (bottom) NMR spectra of 3% $[\text{D}_6]\text{benzene}$ in MBBA samples inside the membrane assembly over a range of temperatures. The signal for dissolved Xe appears between $\delta = 200$ –220 ppm in the ^{129}Xe spectrum. The xenon-in-silicone signal at $\delta = 190$ –196 ppm is not phase corrected for better resolution between it and the dissolved xenon signal and is likely negatively phased as a result of residual suppressed signal. ^2H quadrupolar splitting indicates a transition from an anisotropic to an isotropic phase between 35 °C and 40 °C, in good agreement with the jump in the ^{129}Xe chemical shift of circa 13 ppm for the same temperature range.

Keywords: hyperpolarization · liquid crystals · NMR spectroscopy · phase transitions · xenon

How to cite: *Angew. Chem. Int. Ed.* **2016**, *55*, 4666–4670
Angew. Chem. **2016**, *128*, 4744–4748

- [1] a) L. Schröder, *Phys. Medica* **2013**, *29*, 3–16; b) M. Schnurr, K. Sydow, H. M. Rose, M. Dathe, L. Schröder, *Adv. Healthcare Mater.* **2015**, *4*, 40–45; c) B. Driehuys et al., *Radiology* **2012**, *262*, 279–289; d) S. Patz et al., *Acad. Radiol.* **2008**, *15*, 713–727.
- [2] a) J. Jokisaari, *eMagRes* **2013**, *2*, 279–288; b) P. Sozzani, A. Comotti, R. Simonutti, T. Meersmann, J. W. Logan, A. Pines, *Angew. Chem. Int. Ed.* **2000**, *39*, 2695–2698; *Angew. Chem.* **2000**, *112*, 2807–2810; c) M. A. Springuel-Huet, J. L. Bonardet, A. Gedeon, J. Fraissard, *Magn. Reson. Chem.* **1999**, *37*, S1–S13; d) J. P. Bayle, J. Courtieu, J. Jullien, *J. Chim. Phys.* **1988**, *85*, 147–150; e) M. Baias, D. E. Demco, D. Istrate, C. Popescu, M. Blumich, M. Moller, *J. Phys. Chem. B* **2009**, *113*, 12136–12147; f) M. Duewel, N. Vogel, C. K. Weiss, K. Landfester, H. W. Spiess, K. Munneman, *Macromolecules* **2012**, *45*, 1839–1846; g) I. L. Moudrakovski, A. A. Sanchez, C. L. Ratcliffe, J. A. Ripmeester, *J. Phys. Chem. B* **2001**, *105*, 12338–12347.
- [3] O. Muenster, J. Jokisaari, P. Diehl, *Mol. Cryst. Liq. Cryst.* **1991**, *206*, 179–186.
- [4] a) T. J. Lowery et al., *ChemBioChem* **2007**, *7*, 65–73; b) S. M. Rubin, S.-Y. Lee, E. J. Ruiz, A. Pines, D. E. Wemmer, *Mol. Biol.* **2002**, *322*, 425–440; c) K. K. Palaniappan, R. M. Ramirez, V. S. Bajaj, D. E. Wemmer, A. Pines, M. B. Francis, *Angew. Chem. Int. Ed.* **2013**, *52*, 4849–4853; *Angew. Chem.* **2013**, *125*, 4949–4953; d) C. Boutin et al., *Bioorg. Med. Chem.* **2011**, *19*, 4135–4143; e) M. G. Shapiro, R. M. Ramirez, L. J. Sperling, G. Sun, J. Sun, A. Pines, D. V. Schaffer, V. S. Bajaj, *Nat. Chem.* **2014**, *6*, 629–634; f) Y. Bai, Y. Wang, M. Goulain, A. Driks, I. Dmochowski, *Chem. Sci.* **2014**, *5*, 3197–3203.
- [5] a) A. Schlundt et al., *Angew. Chem. Int. Ed.* **2009**, *48*, 4142–4145; *Angew. Chem.* **2009**, *121*, 4206–4209; b) Q. Wei, G. K. Seward, P. A. Hill, B. Patton, I. E. Dimitrov, N. N. Kuzma, I. J. Dmochowski, *J. Am. Chem. Soc.* **2006**, *128*, 13274–13283; c) T. K. Stevens, R. M. Ramirez, A. Pines, *J. Am. Chem. Soc.* **2013**, *135*, 9576–9579; d) J. A. Finbloom, C. C. Slack, C. J. Bruns, K. Jeong, D. E. Wemmer, A. Pines, M. B. Francis, *Chem. Comm.* **2016**, *52*, 3119–3122.
- [6] S. Klippel, J. Döpfert, J. Jayapaul, M. Kunth, F. Rossella, M. Schnurr, C. Witte, C. Freund, L. Schröder, *Angew. Chem. Int. Ed.* **2014**, *53*, 493–496; *Angew. Chem.* **2014**, *126*, 503–506.
- [7] a) G. Norquay, G. Leung, N. J. Stewart, G. M. Tozer, J. Wolber, J. M. Wild, *Magn. Reson. Med.* **2015**, *74*, 303–311; b) A. Causier, G. Carret, C. Boutin, T. Berthelot, P. Berthault, *Lab Chip* **2015**, *15*, 2049–2054; c) B. M. Goodson, *J. Magn. Reson.* **2002**, *155*, 157–216; d) N. Amor, P. P. Zanker, P. Blumler, F. M. Meise, L. M. Schreiber, A. Scholz, J. Schmiedeskamp, H. W. Spiess, K. Munnemann, *J. Magn. Reson.* **2009**, *201*, 93–99; e) Z. I. Cleveland, H. E. Moller, L. W. Hedlund, B. Driehuys, *J. Phys. Chem. B* **2009**, *113*, 12489–12499.
- [8] a) J. P. Jokisaari, G. R. Luckhurst, B. A. Timimi, J. Zhu, H. Zimmermann, *Liq. Cryst.* **2015**, *1*–14; b) X. Li, C. Newberry, I. Saha, P. Nikolaou, N. Whiting, B. M. Goodson, *Chem. Phys. Lett.* **2006**, *419*, 233–239.
- [9] a) See Ref. [2 f]; b) D. Baumer, E. Brunner, P. Blumler, P. P. Zanker, H. W. Spiess, *Angew. Chem. Int. Ed.* **2006**, *45*, 7282–7284; *Angew. Chem.* **2006**, *118*, 7440–7442.
- [10] D. S. Thiriot, A. A. Nevzorov, S. J. Opella, *Protein Sci.* **2005**, *14*, 1064–1070.
- [11] J. B. Miller, J. H. Walton, C. M. Roland, *Macromolecules* **1993**, *26*, 5602–5610.
- [12] A. Cherubini, A. Bifone, *Prog. Nucl. Magn. Reson. Spectrosc.* **2003**, *42*, 1–30.
- [13] M. H. Levitt, *Spin dynamics: Basics of Nuclear Magnetic Resonance*, Wiley, Hoboken, **2001**.
- [14] J. Karjalainen, J. Vaara, M. Straka, P. Lantto, *Phys. Chem. Chem. Phys.* **2015**, *17*, 7158–7171.
- [15] a) M. D. Croucher, D. J. Patterson, *J. Solution Chem.* **1987**, *144*, 297–307; b) P. H. Keyes, W. B. Daniels, *Mol. Cryst. Liq. Cryst.* **1975**, *63*, 5006–5010.
- [16] E. Molga, J. J. Stecki, *Chem. Thermodyn.* **1977**, *79*–90.
- [17] H. Tsuchiya, K. Nakamura, *Mol. Cryst. Liq. Cryst.* **1974**, *29*, 89–101.

Received: December 11, 2015

Revised: January 26, 2016

Published online: March 8, 2016